AJNR

Persistent Diffusion-Restricted Lesions in Bevacizumab-Treated Malignant Gliomas Are Associated with Improved Survival Compared with Matched Controls

S. Mong, B.M. Ellingson, P.L. Nghiemphu, H.J. Kim, L. Mirsadraei, A. Lai, W. Yong, T.M. Zaw, T.F. Cloughesy and W.B. Pope

AJNR Am J Neuroradiol 2012, 33 (9) 1763-1770
doi: https://doi.org/10.3174/ajnr.A3053
http://www.ajnr.org/content/33/9/1763

ORIGINAL RESEARCH

Persistent Diffusion-Restricted Lesions in Bevacizumab-Treated Malignant Gliomas Are Associated with Improved Survival Compared with Matched Controls

S. Mong
B.M. Ellingson
P.L. Nghiemphu
H.J. Kim
L. Mirsadraei
A. Lai
W. Yong
T.M. Zaw
T.F. Cloughesy
W.B. Pope

BACKGROUND AND PURPOSE: A subset of patients with malignant glioma develops conspicuous lesions characterized by persistent restricted diffusion during treatment with bevacizumab. The purpose of the current study was to characterize the evolution of these lesions and to determine their relationship to patient outcome.

MATERIALS AND METHODS: Twenty patients with malignant glioma with persistent restricted-diffusion lesions undergoing treatment with bevacizumab were included in the current study. Mean ADC and the volume of restricted diffusion were computed for each patient during serial follow-up. Differences in TTP, TTS, and OS were compared between patients with restricted diffusion and matched controls by using Kaplan-Meier analysis with the logrank test and Cox hazard models.

RESULTS: Mean ADC values were generally stable with time (mean, 5.2 ± 12.6% change from baseline). The volume of restricted diffusion increased a median of 23% from baseline by 6 months. Patients with restricted-diffusion lesions had significantly greater TTP (logrank, $P = .013$), TTS (logrank, $P = .008$), and OS (logrank, $P = .010$) than matched controls. When available, advanced physiologic imaging of restricted-diffusion lesions showed hypovascularity on perfusion MR imaging and decreased amino acid uptake on ^{18}F-FDOPA PET scans. Atypical gelatinous necrotic tissue was confirmed in the area of restricted diffusion in 1 patient.

CONCLUSIONS: Restricted-diffusion lesions in malignant gliomas treated with bevacizumab are generally stable with time and are associated with improved outcomes. These results combined with physiologic imaging and histopathologic data suggest that these lesions are not consistent with aggressive tumor.

ABBREVIATIONS: DSC = dynamic susceptibility contrast; ECAT HR = emission computed-assisted tomography high resolution; ^{18}F-FDOPA = fluorine 18 fluorodopamine; Gd-DTPA = gadolinium diethylene triamine pentaacetic acid; KPS = Karnofsky Performance Scale; OS = overall survival; rCBV = relative cerebral blood volume; SEM = standard error of the mean; TTP = time to progression; TTS = time to survival from bevacizumab initiation; WHO = World Health Organization; VEGF = vascular endothelial growth factor

Malignant gliomas, which constitute two-thirds of the 20,500 primary brain malignancies diagnosed annually in the United States, typically progress despite treatment.[1] The median survival after recurrence of WHO grade III gliomas (which include anaplastic astrocytomas, anaplastic oligoastrocytomas, and anaplastic oligodendrogliomas) is 39–40 weeks and 25–30 weeks for WHO grade IV gliomas (glioblastomas).[2] Bevacizumab, a monoclonal antibody targeted against VEGF, is emerging as an alternative or complementary treatment in malignant gliomas.[3] Because antiangiogenic treatment typically decreases the permeability of the blood-brain barrier, its therapeutic application reduces the value of contrast enhancement as a radiographic proxy for tumor response.[4] Alternative MR imaging techniques such as DWI have shown promise in defining both tumor response and nonenhancing tumor progression in the setting of bevacizumab treatment.[5,6]

ADC, a measure reflecting the magnitude of free water mobility obtained by using DWI, can be reduced by the presence of increased cell membranes that typify hypercellular tumor[7,8]; however, ADC can be reduced by other biophysical parameters, including increased viscosity; protein content, such as occurs in abscess[9]; and movement of water from the extraceullar to intracellular space as seen in ischemia or cytotoxic edema.[10] Recently, investigators and clinicians have noted an interesting phenomenon in patients with malignant glioma treated with bevacizumab, consisting of lesions with conspicuously low ADC, which persists over long periods of time.[11-13] While DWI has been used to characterize tumor burden in glioblastoma[14] and to differentiate necrotic cystic brain tumors such as glioblastomas from abscesses,[15] the clinical significance of these persistent restricted-diffusion lesions arising during bevacizumab treatment in malignant gliomas is less straightforward. While some investigations suggest that these lesions reflect hypercellular and aggressive tumor,[11]

Received November 21, 2011; accepted after revision January 17, 2012.

From the Departments of Radiological Sciences (S.M., B.M.E., W.B.P., H.J.K., T.M.Z.), Neurology (T.F.C., A.L., P.L.N.), and Pathology (W.Y., L.M.), David Geffen School of Medicine, University of California, Los Angeles, Los Angeles, California.

This work was supported by the UCLA Institute for Molecular Medicine Seed Grant (B.M.E.), UCLA Radiology Exploratory Research Grant (B.M.E.), Brain Tumor Funders Collaborative (W.B.P.), Art of the Brain (T.F.C.), Ziering Family Foundation in memory of Sigi Ziering (T.F.C.), Singleton Family Foundation (T.F.C.), and the Clarence Klein Fund for Neuro-Oncology (T.F.C.).

Please address correspondence to Whitney B. Pope, UCLA Radiological Sciences, Box 951721, BL-428 CHS, Los Angeles, CA 90095-1721; e-mail: wpope@mednet.ucla.edu

http://dx.doi.org/10.3174/ajnr.A3053

other studies suggest that these lesions represent chronic hypoxia and atypical gelatinous necrotic tissue.[11,12]

The purpose of the current study was to determine the origin of these restricted-diffusion lesions by first characterizing the evolution of restricted-diffusion lesions in malignant gliomas treated with bevacizumab, examining these lesions in a subset of patients with advanced imaging findings and histopathology, and, last, determining the relationship of these lesions with patient outcomes including TTP, TTS, and OS.

Materials and Methods

Patient Selection

This retrospective study was granted a waiver of informed consent by our institutional review board, and all data collection was performed in compliance with Health Insurance Portability and Accountability Act regulations. Prospectively, 24 patients with malignant glioma who developed regions of well-demarcated high signal intensity on diffusion-weighted imaging that also corresponded to regions of reduced ADC values on surveillance imaging were identified by the senior author. Patients were screened for the diagnosis of malignant glioma (WHO grades III and IV), treatment with bevacizumab between January 2007 through August 2011, and a well-circumscribed lesion with restricted diffusion near the original tumor site that persisted for at least 2 months. Patients were required to be older than 18 years of age; have a history of surgical resection, temozolomide administration, and external beam radiation therapy; and have a baseline KPS $\geq$70 at diagnosis. Additional inclusion criteria were accurate reporting of recurrence status, absence of intracranial hemorrhage, and absence of clinical findings or observations of acute or subacute ischemia. Twenty cases were included in the study. As a control cohort, 60 patients with malignant glioma lacking conspicuous diffusion signal abnormality (both the well-circumscribed discrete lesions described above as well as any speckled diffuse pattern of diffusion restriction that can be seen in bevacizumab-treated patients) were collected from our neuro-oncology data base. Controls were matched by sex, age, treatment (bevacizumab), tumor grade, and tumor histology at the time of bevacizumab treatment.

MR Diffusion Image Acquisition and Postprocessing Image Analysis

Patients were imaged on either a 1.5T or 3T clinical MR imaging system, with 50% of patients undergoing all studies on a 1.5T system and 50% of patients undergoing $\leq$2 studies on a 3T scanner and the rest of the studies on a 1.5T scanner (Avanto or Sonata, Siemens, Erlangen, Germany; HDx or LX, GE Healthcare, Milwaukee, Wisconsin) or a 3T scanner (Verio or Trio; Siemens). Anatomic sequences were collected according to standard clinical protocols and included axial precontrast T1-weighted, T2-weighted fast spin-echo, and FLAIR T2-weighted images and Gd-DTPA–enhanced (Magnevist; Berlex, Wayne, New Jersey; 0.1 mmol/kg) axial T1-weighted images acquired after contrast injection. DWI was collected before contrast administration with TE/TR = 90–100/8000–10,000 ms, NEX = 1, section thickness = 3–5 mm with 0- to 1-mm intersection distance, matrix size = 128 × 128 (reconstructed images were zero-padded and interpolated to 256 × 256), and FOV = 24 cm by using a twice-refocused spin-echo–EPI preparation.[16] ADC images were calculated from acquired DWIs with $b = 1000$ s/mm^2 and $b = 0$ s/mm^2 images.

Five patients had dynamic susceptibility perfusion imaging, performed following a preload dose (0.025 mmol/kg) of gadolinium contrast agent to diminish contrast leakage effects, followed by administration of a 3- to 5-mL/s bolus of Gd-DTPA at a dose of 10–20 mL (0.075 mmol/kg) followed by a 20-mL flush of isotonic saline by using a power injector. Parameters used included the following: TE ranging from 23 to 50 ms, TR ranging from 1250 to 1400 ms, flip angles ranging from 30° to 35°, 40–90 repetitions (temporal time points), section thickness ranging from 4 to 7 mm with intersection gap ranging from 0 to 1.5 mm, number of sections ranging from 6 to 20, and matrix size ranging from 80 × 96 to 128 × 128. Postprocessing data analysis was performed to determine standardized rCBV by using previously published methods[17] and commercially available software (IB Neuro v2.0; Imaging Biometrics, Elm Grove, Wisconsin).

^{18}F-FDOPA PET images were obtained for 7 patients as previously described.[18] A high-resolution full-ring ECAT HR or ECAT HR+ PET scanner (CTI-Siemens, Knoxville, Tennessee) was used to acquire images, which contained either 47 contiguous transaxial sections with a section thickness of 3.4 mm (with the ECAT HR) or 63 contiguous transaxial sections with a section thickness of 2.4 mm (axial FOV of 15 cm with the ECAT HR+). After an intravenous injection of 3.5 mCi of ^{18}F-FDOPA, images were acquired immediately with 30-minute emission and 5-minute transmission scans.

Manual regions of interest contouring DWI-hyperintense lesions were obtained by a single observer and verified by 2 independent observers. Mean ADC within the region of interest and volume of the region of interest were extracted on each follow-up time point by using the Analysis of Functional NeuroImages software package (http://afni.nimh.nih.gov/afni). A single 2-mm-diameter circular region of interest was used to sample within the region of diffusion abnormality, and the minimum mean ADC value was recorded for all scan dates for each patient. For advanced imaging studies, color-coded rCBV perfusion maps, and ^{18}F-FDOPA PET scans were registered and compared with a $b = 1000$ s/mm^2 DWI obtained within 2 weeks of rCBV or ^{18}F-FDOPA PET image acquisition.

Statistical Analysis

An unpaired Student *t* test was used to compare the mean ADC values across tumor grades. Linear regression was performed to define the trends in change in mean ADC values with time, and nonlinear regression was performed to define trends in the change in lesion volume with time. The comparison of the change in mean ADC with time and the change in the volume of restricted diffusion with time with survival outcomes was analyzed by using Kaplan-Meier analysis with a logrank test and Cox hazard models. Survival analysis comparing outcomes including TTP and TTS and OS from the initial diagnosis was performed to compare patients with controls.

Results

The demographic, clinical, and treatment characteristics of the 20 patients are summarized in the Table. Of the patients with restricted-diffusion lesions, 14 (70%) had glioblastomas. Most patients (70%) underwent subtotal resection or attempted gross total resection.

Most controls (85%) also had glioblastomas. Both patients and controls demonstrated baseline KPS of >70. Most patients (70%) and controls (79%) underwent subtotal resection or attempted gross total resection. Of the 15 (75%) patients with restricted-diffusion abnormalities that developed after initiation of bevacizumab, restricted diffu-

Patient characteristics at onset of restricted-diffusion lesion		
	Cases	Controls
Total patients	20	60
Age (median) (range)(yr)	51 (20–82)	54 (21–82)
Sex (male/female)	12:8	36:24
Diagnosis		
Glioblastoma	14 (70%)	51 (85%)
Anaplastic astrocytoma	4 (20%)	5 (8%)
Anaplastic oligodendroglioma	2 (10%)	1 (2%)
Anaplastic mixed glioma	0 (0%)	3 (5%)
Histologic grade		
III	6	9
IV	14	51
Initial KPS (mean) (range)	87 (70–100)	82 (60–100)
Extent of resection		
0%–10%	6 (30%)	13 (21%)
11%–89%	8 (40%)	22 (37%)
90%–100%	6 (30%)	25 (42%)
Recurrence status at time of lesion onset		
New	4 (20%)	16 (27%)
First	9 (45%)	30 (50%)
Second	3 (15%)	11 (18%)
Third	4 (20%)	3 (5%)

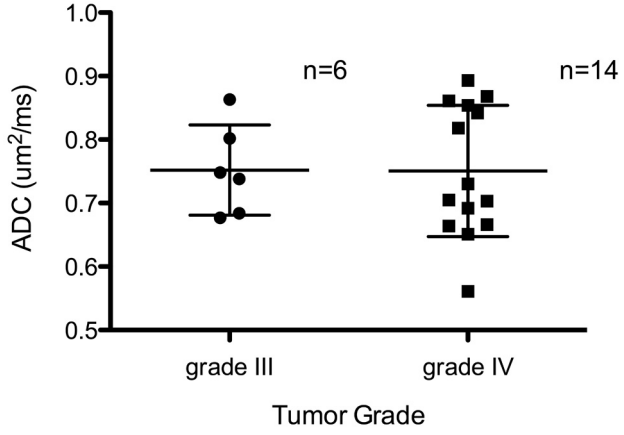

Fig 1. Mean ADC from diffusion-restricted abnormality is stratified by tumor grade, with the SD shown.

sion was noted an average of 232 days (SEM, 51.5 days) after bevacizumab treatment, and it persisted for 403 days (SEM, 98 days) from lesion onset. A quarter of patients developed restricted diffusion a mean of 55 ± 35 days before initiation of bevacizumab treatment (range, 1–84), with lesions lasting a mean of 409 days (SEM, 89) from lesion onset, with duration and evolution that was similar to those of the rest of the cohort (unpaired Student *t* test, $P = .97$). When we took all patients together, the restricted-diffusion lesions lasted a mean of 404 days (SEM, 76). Lesions developed in the setting of recurrent disease in 16 patients (80%) and 44 controls (73%).

Mean ADC was not significantly different across tumor grades ($P = .97$, unpaired *t* test) (Fig 1). The minimum mean ADC value measured from a circular region of interest with a diameter of 2 mm from within the region of diffusion abnormality was 0.44 μm^2/ms (SEM, 0.02 μm^2/ms). The mean ADC value increased an average of 5.2% during 6 months from a stable baseline measured within 1 month of the onset of the lesion (SEM, 2.8%). Mean ADC values did not vary when the patients were stratified by scanner strength ($P = .998$). Linear regression revealed that 13 patients (65%) had no significant change from baseline ADC values with time. Meanwhile, the lesion volume increased a median of 23.3% over baseline during the same 6-month period. Lesion volume remained stable in 18 patients (90%), with only 2 demonstrating a doubling of median lesion volume during 6 months. Regardless of whether diffusion signal abnormalities developed before or after bevacizumab treatment, lesions remained stable in size from the time of the first presentation to >1 year afterward (Fig 2).

Localization of restricted-diffusion lesions near the ventricles and the corpus callosum was most common, because 19 lesions (95%) were adjacent to the ventricles and 11 lesions (55%) involved both the periventricular region and the corpus callosum. Additionally, 18 patients (80%) developed lesions that demonstrated faint spontaneous T1-weighted hyperintense rims. These T1 characteristics were visible for a year in all 9 patients (50%), with surveillance up to 1 year after lesion onset.

We next determined that the presence of restricted-diffusion lesions predicted improved survival outcomes. Patients with restricted-diffusion lesions had significantly greater TTP compared with matched controls (Fig 3; logrank, $P = .013$), with a median TTP of 248 days (95% confidence interval, 155–389 days) versus 159 days (95% confidence interval, 122–227 days), respectively. Similarly, patients with restricted-diffusion lesions had significantly greater TTS compared with matched controls (logrank, $P = .008$), demonstrating a median TTS of 596 days (95% confidence interval, 425–1395 days) versus 348 days (95% confidence interval, 257–390 days), respectively. Patients with restricted-diffusion lesions also had greater OS compared with matched controls (logrank, $P = .010$), illustrating a mean OS of 1676 days (95% confidence interval, 639–3141 days) versus 633 days (95% confidence interval, 559–765 days), respectively. While positive change in mean ADC with time trended toward longer TTP and TTS compared with stable or decreasing temporal changes in mean ADC, this was not statistically significant ($P = .15$, logrank; $P = .11$, logrank, respectively). Similarly, an increasing volume of restricted diffusion with time trended toward a shorter TTS compared with patients demonstrating stable or decreasing volume ($P = .08$, logrank).

In cases with advanced physiologic imaging, regions of diffusion signal abnormality were hypoperfused in 5 of 6 patients and showed decreased amino acid uptake on ^{18}F-FDOPA PET scans in 7 of 8 patients (Fig. 4). Examination of the nine ^{18}F-FDOPA PET scans and 3 perfusion scans available for controls demonstrated avidity and hyperperfusion at the site of tumor in all patients. Recurrent tumor was found in the 6 controls with histology available (data not shown), and gelatinous necrotic tissue was found within the diffusion abnormality during surgical resection in 1 patient (Fig. 5). Histologic examination of this case demonstrated prominent fibrosis of the vasculature amid diffuse necrotic changes.

Discussion

Previous investigations examining the development of conspicuous restricted-diffusion lesions in patients with malignant glioma treated with antiangiogenic therapy have suggested that these lesions may reflect aggressive infiltrative

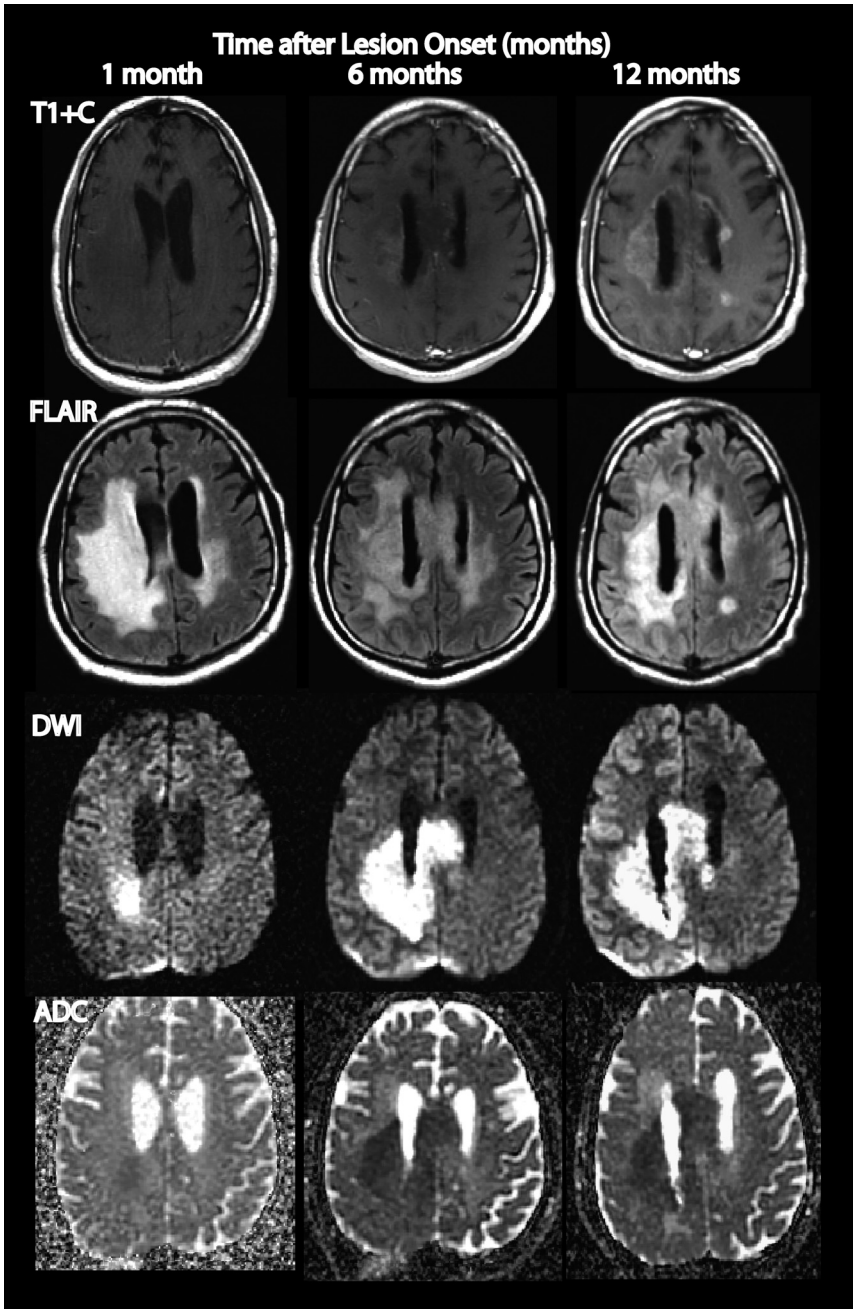

Fig 2. In a patient with glioblastoma with a well-defined and discrete diffusion-restricted lesion that developed before bevacizumab treatment, the lesion is shown at 1 month after its presentation and remains stable in size at 6 months and 1 year afterward. T1-weighted postcontrast image shows FLAIR hyperintensity and faint rim enhancement by 1 year.

tumor.[7] Conversely, others have suggested that these persistent restricted-diffusion lesions may correspond to areas of atypical necrosis in the setting of anti-VEGF treatment-induced chronic hypoxia.[9] In the current study, we have built on previous studies by characterizing the time-dependent changes in these lesions and determining whether these patients differ with respect to patient outcomes compared with carefully matched controls. Specifically, we focused on determining whether the presence of restricted-diffusion lesions was associated with decreased survival (as would be expected for progressive infiltrative tumor) or improved survival (as would be hypothesized for areas of necrosis and treatment effect) compared with controls.

The current study suggests that restricted-diffusion lesions do not significantly change in the degree of restriction (ADC value) or volume of abnormality for up to 6 months after lesion onset following bevacizumab treatment. Thirteen patients (65%) did not demonstrate significant change of mean ADC values from baseline values at lesion onset. Similarly, the volume of restricted-diffusion lesions remained stable in most patients (90%), with 1 lesion showing no significant change in size or appearance during 2 years of subsequent surveillance in the patient with the longest imaging follow-up available. We incidentally noted that these lesions clustered around the lateral ventricles and frequently involved the corpus callosum, with the latter similar in incidence as reported in a previous case series.[13] The restricted periventricular distribution may be less typical of growing tumor than of therapy-induced ne-

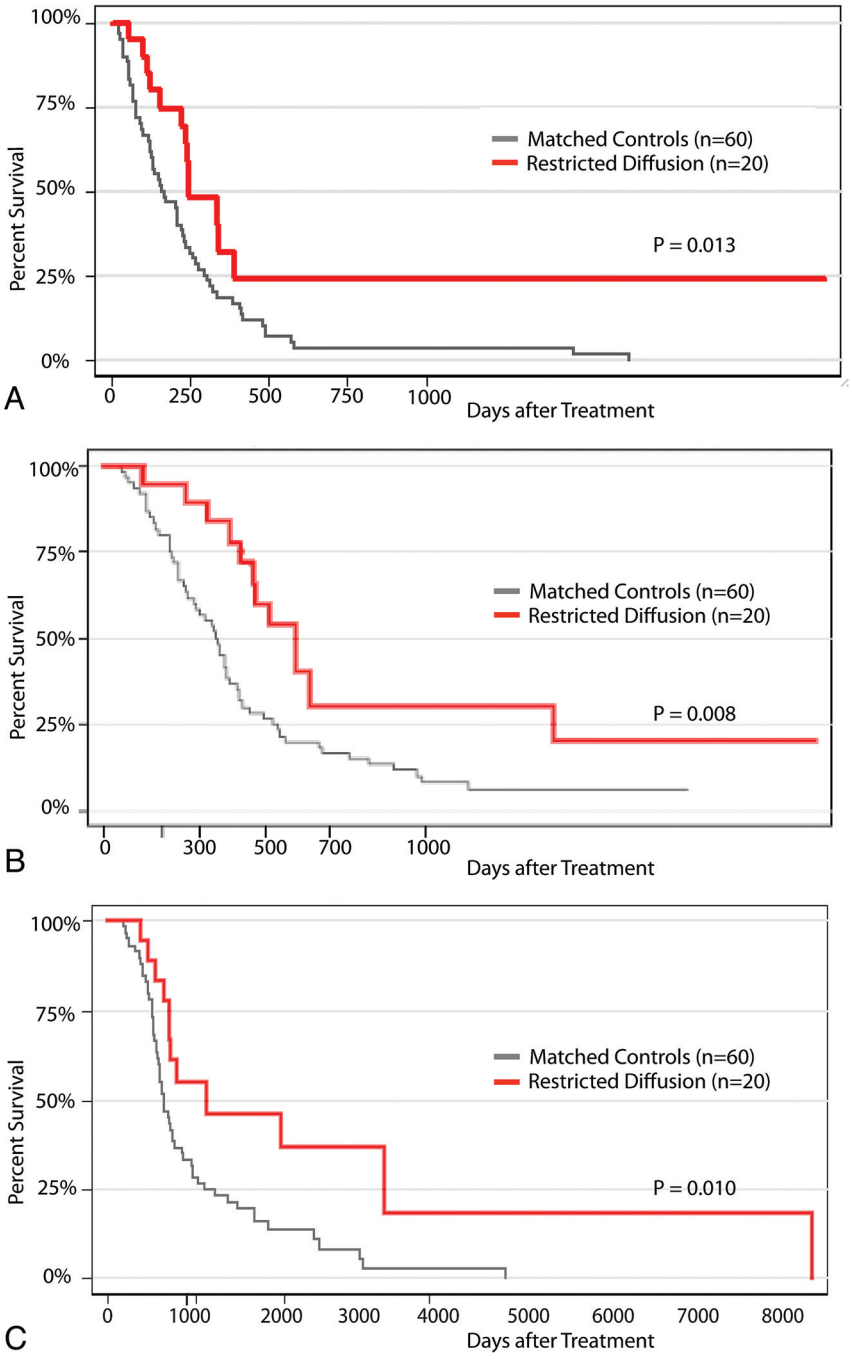

Fig 3. Time to progression (*A*), time to survival (*B*), and overall survival (*C*) are calculated by using Kaplan-Meier curves to compare outcomes for patients with restricted-diffusion abnormalities with those for matched controls.

crosis.[19] Most interesting, these lesions also illustrated a faint rim of spontaneous T1-weighted hyperintensity on precontrast T1-weighted images but not the prominent rim enhancement or internal T2 signal approaching CSF that is typical for necrotic areas on MR imaging. Similar to a previous case report,[12] in patients with DSC perfusion MR imaging ($n = 5$), regions of restricted diffusion corresponded spatially with abnormally low rCBV, lower than both tumor and normal-appearing white matter. Application of ^{18}F-FDOPA PET scans in 7 patients demonstrated no abnormal tracer uptake compared with normal-appearing white matter.

Additionally, the minimum mean ADC signal measured within these restricted-diffusion lesions was lower than would be expected from viable biologic tissue. For example, 1 patient with recurrent glioblastoma had a minimum mean ADC of 0.33 μm^2/ms, which is much lower than the range of minimum ADC values reported for actively growing tumor (0.77–1.4 μm^2/ms).[20] The value reported in our study is also lower than the range reported for a cohort of patients with glioblastoma, in whom approximately half were treated with bevacizumab and who also developed restricted-diffusion abnormalities (0.44–0.97 μm^2/ms).[13] We hypothesized that these low ADC values may be characteristic of this atypical necrosis. In 1 patient who underwent complete surgical resection of a

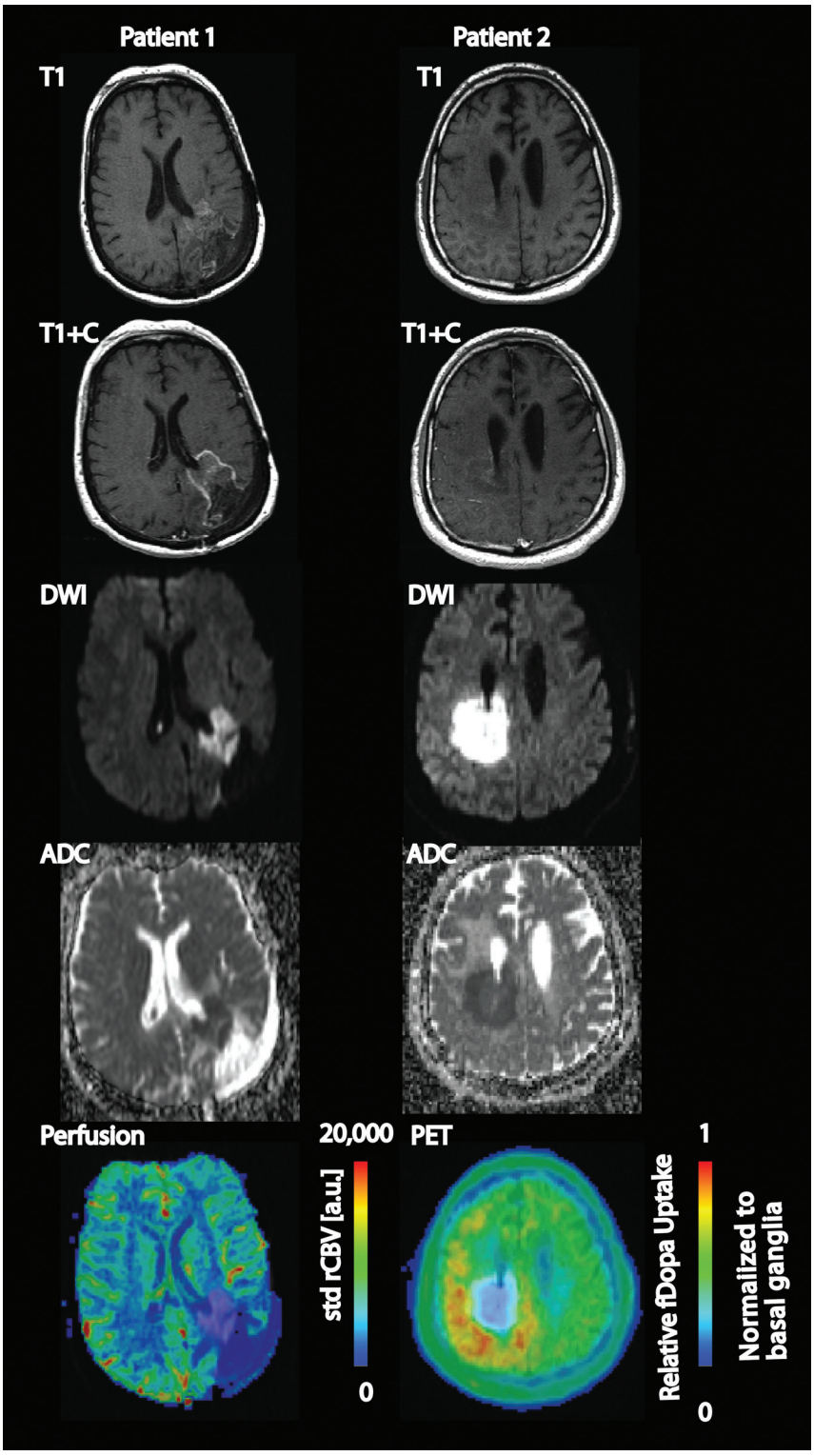

Fig 4. A representative low ADC lesion in a patient with glioblastoma demonstrates faint rim-enhancement on T1-weighted MR imaging with and without contrast, low signal intensity on ADC, hyperintensity on DWI, and hypermetabolic activity on ^{18}F-FDOPA PET scans. The standardized rCBV in the region of interest (normalized to normal-appearing white matter) was 0.44 in this patient. The legend shows standardized rCBV scaled 0–20,000 astronomical units. Another representative lesion demonstrates the above features, as well as hypoperfusion on a DSC perfusion MR imaging. The legend shows relative ^{18}F-FDOPA uptake with the standardized uptake value (SUV) normalized to basal ganglia, with the mean SUV in this patient of 0.43.

large diffusion-restricted lesion, histopathologic examination of the specimen confirmed atypical necrosis, similar to that in a previous case report.[12] With this additional radiologic-histologic correlation, the degree of diffusion restriction may be developed as a useful tool to differentiate necrosis from tumor recurrence.

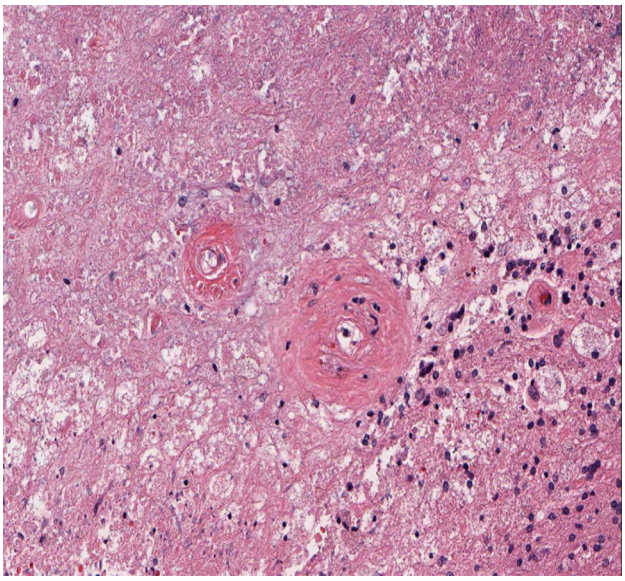

Fig 5. Neuropathologic evaluation of a biopsy specimen from the area of diffusion restriction demonstrates an area of necrosis on the hematoxylin-eosin staining. Fibrotic changes of blood vessels are prominent (original magnification, ×200).

While most patients with recurrent malignant glioma with baseline local, diffuse, multifocal, or distant disease at recurrence later demonstrated these same patterns of tumor spread at the time of progression,[21] correlating the different radiographic patterns of progression with histopathology and ADC values may provide insight into the distinction between diffusion signal abnormality associated with treatment effect and that associated with infiltrating tumor. In this study, the relatively slow changes in volume and mean ADC, the minimum ADC values that are much lower than is consistent with growing tumor, and the survival advantage in patients who develop persistent restricted-diffusion lesions, combined with the hypovascular and hypometabolic findings on perfusion MR imaging and ^{18}F-FDOPA PET, respectively, are most compatible with nonviable tissue rather than active tumor.

Study Limitations

The variation within this small cohort of patients with respect to tumor histology, recurrence status at time of bevacizumab initiation, and treatment protocols before bevacizumab administration are potential limitations to the current study. Despite this heterogeneity, the presence of these lesions demonstrated a prolonged survival independent of histologic grade, recurrence status, and treatment history preceding bevacizumab administration. The frequency of MR follow-up imaging was limited in a few cases but was sufficient to demonstrate stability in the ADC signal intensity with time. This lack of consistent follow-up times is also a potential limitation because more complete and more frequent longitudinal imaging follow-ups would permit more accurate tracking of trends in the change in mean ADC signal with time, for further correlation with survival outcomes.

Another limitation to the current study was the lack of histologic validation, which was not possible for most patients because of the retrospective nature of the current study and because resection was not included during their routine care at recurrence. Instead, advanced imaging correlates were used to corroborate the hypothesis that these lesions represent treatment effect rather than tumor progression. Additional histologic examinations of biopsies taken from the site of diffusion restriction are necessary to definitively clarify the etiology of these lesions. Because it is clear that these restricted-diffusion abnormalities may develop both in and outside the setting of bevacizumab treatment, a larger sample or pooling of cases across institutions is necessary to perform a more detailed characterization and segmentation of patients with this phenotype.

Conclusions

Imaging and survival data from the current study converge to further support the hypothesis that the development of geographic well-defined regions of persistent diffusion restriction after bevacizumab treatment in patients with malignant gliomas is not associated with growing tumor but rather may be related to atypical necrosis in many patients. Such lesions can be identified on the basis of a low minimum ADC value, atypical well-circumscribed appearance on T1-weighted MR images, and a characteristic location in paraventricular white matter regions.

Disclosures: Leia Nghiemphu—*RELATED*: *Consulting Fee or Honorarium*: Genentech Inc, *Comments*: Honorarium. Albert Lai—*RELATED*: *Grant*: Genentech/Roche,* *Comments*: research grant for correlative tissue analysis related to bevacizumab use, *UNRELATED*: *Consultancy*: Genentech/Roche, *Comments*: Scientific Advisory Board. William Yong—*UNRELATED*: *Other*: Collaborations with Genentech.* Timothy Cloughesy—*RELATED*: *Consulting Fee or Honorarium*: Roche, Genentech, *Fees for Participation in Review Activities (such as data monitoring boards, statistical analysis, end point committees, and the like)*: Roche, *UNRELATED*: *Consultancy*: Merck, Novartis, *Payment for Lectures (including service on speakers bureaus)*: Merck. Whitney Pope—*RELATED*: *Consulting Fee or Honorarium*: Genentech, *UNRELATED: Consultancy*: Genentech. *Money paid to the institution.

References

1. Norden AD, Drappatz J, Wen PY. **Antiangiogenic therapies for high-grade glioma.** *Nat Rev Neurol* 2009;5:610–20
2. Quant EC, Drappatz J, Wen PY, et al. **Recurrent high-grade glioma.** *Curr Treat Options Neurol* 2010;12:321–33
3. Friedman HS, Prados MD, Wen PY, et al. **Bevacizumab alone and in combination with irinotecan in recurrent glioblastoma.** *J Clin Oncol* 2009;27:4733–40
4. Ellingson BM, Cloughesy TF, Lai A, et al. **Quantitative volumetric analysis of conventional MRI response in recurrent glioblastoma treated with bevacizumab.** *Neuro Oncol* 2011;13:401–09
5. Ellingson BM, Cloughesy TF, Lai A, et al. **Graded functional diffusion map-defined characteristics of apparent diffusion coefficients predict overall survival in recurrent glioblastoma treated with bevacizumab.** *Neuro Oncol* 2011;13:1151–61
6. Ellingson BM, Cloughesy TF, Lai A, et al. **Cell invasion, motility, and proliferation level estimate (CIMPLE) maps derived from serial diffusion MR images in recurrent glioblastoma treated with bevacizumab.** *J Neurooncol* 2011;105:91–101
7. Ellingson BM, Malkin MG, Rand SD, et al. **Validation of functional diffusion maps (fDMs) as a biomarker for human glioma cellularity.** *J Magn Reson Imaging* 2010;31:538–48
8. Sadeghi N, D'Haene N, Decaestecker C, et al. **Apparent diffusion coefficient and cerebral blood volume in brain gliomas: relation to tumor cell density and tumor microvessel density based on stereotactic biopsies.** *AJNR Am J Neuroradiol* 2008;29:476–82
9. Luthra G, Parihar A, Nath K, et al. **Comparative evaluation of fungal, tubercular, and pyogenic brain abscesses with conventional and diffusion MR imaging and proton MR spectroscopy.** *AJNR Am J Neuroradiol* 2007;28:1332–38
10. Somford DM, Marks MP, Thijs VN, et al. **Association of early CT abnormalities, infarct size, and apparent diffusion coefficient reduction in acute ischemic stroke.** *AJNR Am J Neuroradiol* 2004;25:933–38

11. Gerstner ER, Frosch MP, Batchelor TT. **Diffusion magnetic resonance imaging detects pathologically confirmed, nonenhancing tumor progression in a patient with recurrent glioblastoma receiving bevacizumab.** *J Clin Oncol* 2010;28:e91–93
12. Rieger J, Bahr O, Muller K, et al. **Bevacizumab-induced diffusion-restricted lesions in malignant glioma patients.** *J Neurooncol* 2010;99:49–56
13. Gupta A, Young RJ, Karimi S, et al. **Isolated diffusion restriction precedes the development of enhancing tumor in a subset of patients with glioblastoma.** *AJNR Am J Neuroradiol* 2011;32:1301–06
14. Hakyemez B, Erdogan C, Yildirim N, et al. **Glioblastoma multiforme with atypical diffusion-weighted MR findings.** *Br J Radiol* 2005;78:989–92
15. Chiang IC, Hsieh TJ, Chiu ML, et al. **Distinction between pyogenic brain abscess and necrotic brain tumour using 3-Tesla MR spectroscopy, diffusion and perfusion imaging.** *Br J Radiol* 2009;82:813–20
16. Reese TG, Heid O, Weisskoff RM, et al. **Reduction of eddy-current-induced distortion in diffusion MRI using a twice-refocused spin echo.** *Magn Reson Med* 2003;49:177–82
17. Bedekar D, Jensen T, Schmainda KM. **Standardization of relative cerebral blood volume (rCBV) image maps for ease of both inter- and intrapatient comparisons.** *Magn Reson Med* 2010;64:907–13
18. Ledezma CJ, Chen W, Sai V, et al. **18F-FDOPA PET/MRI fusion in patients with primary/recurrent gliomas: initial experience.** *Eur J Radiol* 2009;71:242–48
19. Rogers LR, Gutierrez J, Scarpace L, et al. **Morphologic magnetic resonance imaging features of therapy-induced cerebral necrosis.** *J Neurooncol* 2011;101:25–32
20. Yamasaki F, Kurisu K, Satoh K, et al. **Apparent diffusion coefficient of human brain tumors at MR imaging.** *Radiology* 2005;235:985–99
21. Pope WB, Xia Q, Paton VE, et al. **Patterns of progression in patients with recurrent glioblastoma treated with bevacizumab.** *Neurology* 2011;76:432–37